



# Development of Viscoelastic Damper System to Improve Seismic Performance of Storage Racks

Gwanghee Heo<sup>1a</sup>, Hyongsuk Choi<sup>1b</sup>, Eunrim Baek<sup>1b</sup>, and Chunggil Kim<sup>1a</sup>

<sup>a</sup>Member, Public Safety Research Center, Konyang University, Nonsan 32992, Korea

<sup>b</sup>Seismic Research and Test Center, Pusan National University, Yangsan 50612, Korea

## ARTICLE HISTORY

Received 5 June 2020  
Revised 1st 6 November 2020  
Revised 2nd 19 January 2021  
Accepted 12 April 2021  
Published Online 18 June 2021

## KEYWORDS

Storage racks  
Shaking table test  
Viscoelastic damper  
Seismic safety  
Seismic reinforcement  
Seismic resistance

## ABSTRACT

Storage racks are nonstructural components mainly designed to support the vertical load of goods. During strong external loads such as an earthquake, which acts in the lateral direction of the racks, stored goods become structurally vulnerable. To identify and reinforce the vulnerable parts of storage racks and improve their seismic performance, we developed a viscoelastic damper system with a capacity designed for storage racks. First, we performed an experiment to analyze the behavioral characteristics of a pallet rack — a representative storage rack used for large goods — under vibration. Based on the results of the experiment, we chose the members of storage racks that were vulnerable to vibration. For the proper seismic reinforcement of vulnerable members, we developed a viscoelastic damping system for storage racks by calculating the structural shear force on each floor of the rack and the capacity of the damper to distribute the shear force. First, three viscoelastic dampers of different capacities were fabricated using a viscoelastic material and subjected to cyclic loading tests to evaluate their mechanical performance. We determined the position on which the damper should be placed to improve the rack's seismic performance by considering the shear force on each floor of the storage rack and its operational characteristics. Finally, we conducted a shaking table test to verify the new viscoelastic damper system. The system improves the seismic performance of storage racks by controlling their elastic and permanent deformations.

## 1. Introduction

Storage racks are representative nonstructural components that are designed and fabricated to support heavier loads than their own weight. Widely used in logistics, storage racks can be easily assembled using columns, beams, and bracing. In particular, beams on which goods are stored are connected to columns, which play the role of transferring the load to the ground (vertical direction) using simple hooks. This connection method allows free space configuration and easy assemblage. However, it often brings structural instability, such as damage to hooks, and collapses in the lateral direction due to a strong lateral external force (FEMA 460, 2005).

Severe damage to storage racks in a logistics center caused by the 1994 LA Northridge (US) earthquake fueled interest in the seismic engineering of storage racks. Manuals on the installation

of various types of storage racks, such as FEMA 460 in the US and FEM in Europe, have been produced, and guidelines on their installation and operation have been presented (FEM 10.2.02., 2000; FEMA 460, 2005; EN 1993-1-3, 2006; Building Seismic Safety Council, 2009; EN 15512, 2009; FEM 10.2.08, 2010; ANSI MH16.1, 2012). Researchers have also conducted studies on storage racks to improve the guidelines that did not guarantee sufficient seismic performance (Markazi et al., 1997; Bernuzzi and Castiglioni, 2001; de Lima et al., 2002; Castiglioni et al., 2003; Kozłowski and Slecza, 2004; Bajoria and Talikoti, 2006; Slecza and Kozłowski, 2007; Filiatrault et al., 2007; Bograd et al., 2011; Eriten et al., 2013; Castiglioni, 2016). Existing studies on storage facilities explored the following areas: modeling of the vulnerable elements of storage racks, finite element modeling for analyzing the behavioral characteristics of storage racks, and the effect of connections on the behavior of storage racks under seismic

**CORRESPONDENCE** Chunggil Kim ✉ cg-kim@konyang.ac.kr ☒ Public Safety Research Center, Konyang University, Nonsan 32992, Korea

© 2021 Korean Society of Civil Engineers

loads.

As for studies on the analysis of vulnerable elements of storage racks, Krawinkler et al. (1978) conducted an experimental research on 20 storage rack connections (column–beam connections) using cantilevers. In that experiment, columns and beams were connected using hooks or button grips to evaluate the effect of the connection method on the vulnerability of storage racks. The results confirmed that low-cycle fatigue could affect the strength and ductility of connections. Bernuzzi and Castiglioni (2001) conducted the cyclic loading test on two types of connections with different hole and hook types, to examine the effect of the operation of column–beam connections on the overall behavior of storage racks. The hooks and connection sections were deformed, and the types of load and connection affected the behavior of the connections. In particular, they concluded that the slip phenomenon that occurred in the gap of the connections may be the cause of the large deformation in the storage racks under external loads, such as earthquakes.

A few researchers have analyzed the behavioral characteristics of storage racks using finite element modeling. For example, Chen et al. (1980a; 1980b) proposed a nonlinear  $M$ – $\theta$  hysteresis law using numerical modeling to analyze the seismic performance of storage rack connections. They also verified the accuracy of the two-dimensional nonlinear numerical model in simulating the behavior of storage racks by comparing its response with the results of a shaking table test. They proposed the application of the spring constant in simulating the drift occurring at the connections of storage racks. They found that the spring constant could not accurately simulate low-amplitude natural cycles. Abdel-Jaber et al. (2005) introduced an appropriate correction equation to measure the rotation of the beam that affects the connection under external force, based on the assumption that the column–beam connection is in the elastic state, and compared the performance of the developed model in simulating the connection movement with that of the model based on FEM and SEMA codes. Although the developed model could accurately simulate the moment and deflection of the connection compared with the FEM/SEMA-based model, it could not reflect the moment-reversal phenomenon that occurred during the experiment.

Researchers have also studied the effect of connections on the behavior of storage racks under seismic loads. For example, Beale and Godley (2004) analyzed the shaking of storage racks and confirmed that significantly large moment, rotation, and displacement occurred depending on the top or bottom positions of the connections. Kwarteng et al. (2012) conducted cyclic loading tests on the column–beam connection. They found that the strength of the connection remained constant regardless of the increase in load, despite the rotation angle of the connection having increased after a sudden reduction in the stiffness due to the damage incurred by the connection. They recommended engineers increase the safety factor of the entire structure for the connection to absorb and redistribute energy. Shah and Suhasini (2015) recognizes that the beam-column connection has the main effect on the down-aisle direction shaking, a double

cantilever test was conducted to study the behavior of the connection part, and breakage of the tap and slot of the connection part was confirmed. Jovanovi et al. (2019) determines that beam-column connections are the main factor of down-aisle direction resistance of storage racks, proposes beam-column connections model.

From these studies, the column–beam connections of storage racks have a significant impact on the latter's damage and dynamic behavioral characteristics, which in turn determine the overall performance of the storage racks. Nevertheless, to the best of the authors' knowledge, the measures implemented by these studies to improve the structural safety of the lateral behavior of storage racks are still insufficient. Most performance-enhancing dampers are bulky and manufactured for a large group of storage racks. As such, the literature does not have adequate studies that feature methods to improve the structural performance of individual dampers or a small group of storage racks.

In this study, we developed a viscoelastic damper system to improve the seismic performance of storage racks by reinforcing the vulnerable elements. To this end, we examined the vulnerable elements of storage racks under seismic loads through experiments. The controlling force of the viscoelastic damper in the system was determined by considering the shear force on each floor of the storage rack, and the geometry of the system was designed to minimize interference with the loading of goods in the rack. Mechanical performance tests and shaking table tests were conducted to verify the performance of the damper system. Finally, the effect of the system in improving the seismic performance of the rack was examined by analyzing its contribution to the reduction of elastic and permanent deformation.

## 2. Configuration of a Basic Storage Rack and Analysis of Its Behavioral Characteristics

### 2.1 Configuration of a Basic Storage Rack

This study aimed to develop a viscoelastic damper system to improve the seismic performance of storage racks by increasing their lateral safety under seismic loads. Pallet racks (hereafter, storage racks), which have been most commonly used worldwide, were selected as the target storage racks for such development. For storage racks, the down-aisle direction is open for the loading of goods and the cross-aisle direction is closed with bracing that connects columns as shown in Fig. 1. The space in the down-aisle direction is relatively larger than that in the cross-aisle direction. In the case of storage racks for loading pallets, space for loading two pallets is generally secured. The height of each floor can be adjusted for the convenience of the user. Storage racks have different cross-sectional areas and types depending on the manufacturer, but consist of beams for loading goods, columns that support the beams, and bracing that connects columns in the cross-aisle direction. The beams are connected with the columns using the holes in the columns and the hooks of the beams to freely adjust the height of the beams for the convenience of the user. Anchor bolts are usually used for the

connection between the columns and the floor, but there is no regulation on this connection. Thus, the connection method can be determined by the user.

The viscoelastic damper system in this study increases the lateral safety of storage racks under seismic loads, thereby improving their resistance to earthquakes. Pallet racks (hereinafter, storage racks), which are the most common type of storage shelves, were chosen for this research. For the storage rack design, we kept the down-aisle direction open for the loading of goods while closing

the cross-aisle direction with bracing members that connect the columns, as shown in Fig. 1. The space in the down-aisle direction is larger than that in the cross-aisle direction. In the case of storage racks for loading pallets, the space required for loading two pallets is generally secured. The height of each floor can be adjusted according to the user's convenience. The cross-sectional areas and types of storage racks vary with the manufacturer. However, the common elements of a storage rack include beams for loading goods, columns to support the beams, and bracings

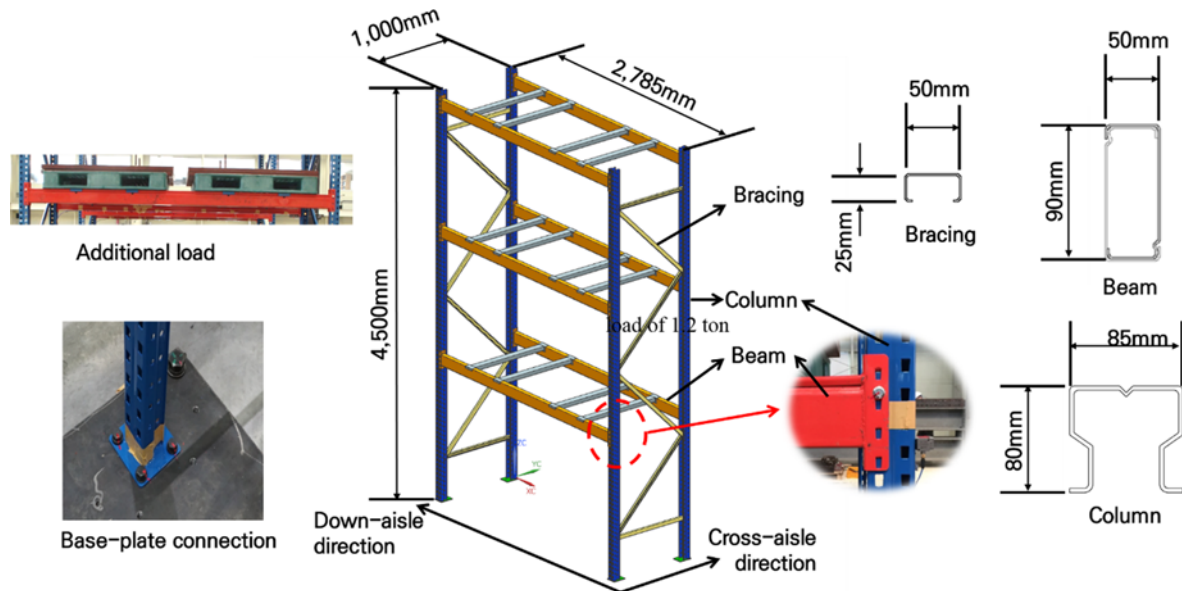


Fig. 1. Configuration and Dimensions of the Storage Rack

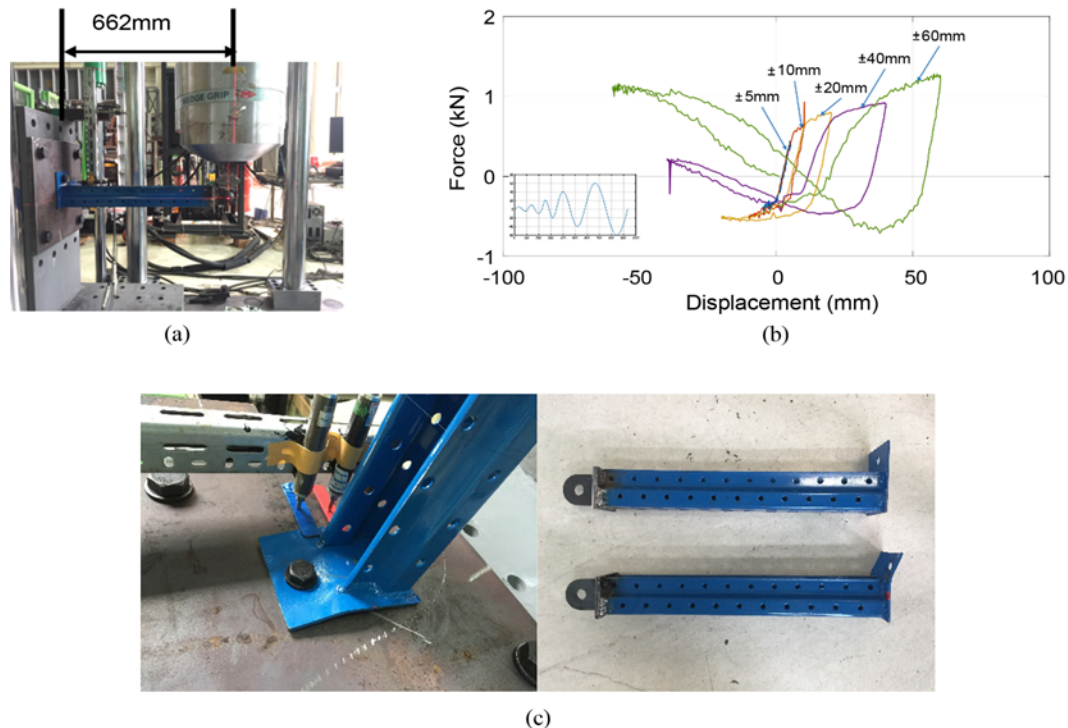


Fig. 2. Base-Plate Connection Test: (a) Set Up for Base-Plate Connection Test, (b) Test Results, (c) Damaged of Plate

that connect columns in the cross-aisle direction. The hook of a beam is inserted into the hole of a column, forming a connection that allows to freely adjust the beam height. Anchor bolts were used to fasten the columns to the floor. However, since there are no specifications for this type of connection, the user may choose their own connection method.

As shown in Fig. 1, the length of the storage rack (down-aisle direction) is 2,785 mm. The width of the rack (cross-aisle direction) is 1,000 mm. The height of the rack is 4,500 mm. In addition, for the experiment on the structural seismic performance of the storage rack, we applied a load of 1.2 ton each floor, which corresponds to 80% of the maximum design load (1.5 t). The application of the load caused the beams to bend. The 80% limit was chosen to exclude the influence of initial bending during the experiment. Two load blocks of 0.3 ton were arranged for each palette and two were placed on each floor in storage rack. As shown in the picture, the column is a thin channel-shaped cross section compared to the length, and the beam is a structure in which two L-shaped cross sections are combined. In general, the storage racks have different connection conditions between the column and the base according to the user's needs. As the most commonly used connection conditions, the base-plate connection test was conducted as shown in Fig. 2, and the deformation of the column plate due to external force was confirmed.

Figure 2 is showing the displacement and force relationship of the rack column specimen by the cyclic loading test in accordance with ANSI/RMI MH16.1 specification. The results of the test showed that the plate damage was confirmed as seen in Fig. 2(c). The base plate of the column was fixed to the shaking table with four M24 bolts to prevent movement and bending of the base plate generated during the experiment. The column-beam connections were fastened with M8 bolts to prevent the beams from unwinding and falling out during the experiment. The rest of the connections were fastened with M10 bolts. For the test specimen, the storage racks were fabricated using cold-worked steel members made of general SS275 steel (KS D 3503).

## 2.2 Experiments and Results: Vibration Characteristics of Storage Rack

For the development of a viscoelastic damper system, we used a shaking table to analyze the vibration characteristics of the storage rack under external loads. The shaking table test of the actual structure was conducted in accordance with the Acceptance Criteria for Seismic Certification by Shake-table Testing of Nonstructural Components proposed by ICC-ES (AC156:2010, 2015), a representative nonstructural component test method. According to the Korea Building Code (KBC, 2016), storage racks are classified as structures other than buildings, but their design loads can be determined by considering them as nonstructural components, if the weight including the building and storage racks is less than 25% of the weight of the structure that supports the storage racks. For this reason,  $S_{DS}$  ( $=0.36575$ ) was calculated by referring to the criteria of KBC2016 for the response spectrum required by the experiment and by assuming

**Table 1.** Parameter for Required Response Spectrum (KBC, 2016)

Building code	$S_{DS}$	$z/h$	Horizontal		Damping
			$A_{FLX-H}$ (g)	$A_{RIG-H}$ (g)	
KBC2016	0.37	0	0.37	0.15	5%

$S_{DS}$ : Design spectral response acceleration at short period

$A_{FLX-H}$  (g): Horizontal spectral acceleration calculated for flexible

$A_{RIG-H}$  (g): Horizontal spectral acceleration calculated for rigid

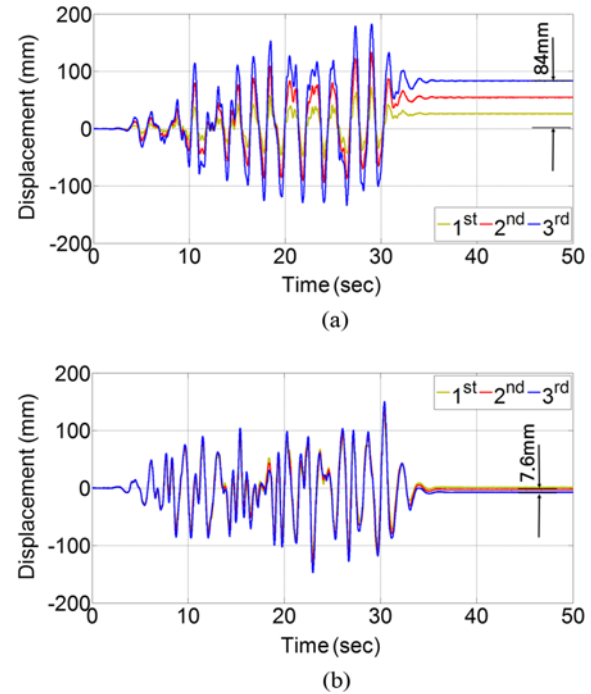


**Fig. 3.** Displacement Responses of Each Floor of the Storage Rack due to External Force: Displacement Responses in the: (a) Down-Aisle Direction, (b) Cross-Aisle Direction

that the storage rack was installed on the ground floor ( $z/h = 0$ ) of a moderate rock ground in seismic zone I. Table 1 shows the parameters used to determine the required response spectrum.

The shaking table test was conducted by increasing the peak ground acceleration (PGA) from the 50% level to the 200% level, based on the PGA ( $= 0.15$  g) of the seismic waveform generated using the required response spectrum information in Table 1. Fig. 3 illustrates the displacement responses of each floor in the down-aisle and cross-aisle directions obtained through the shaking table test.

As shown in Fig. 3, displacement responses along the width (cross-aisle direction, which is smaller than the height and length, were smaller than those along the length (down-aisle direction). This may be because no reinforcement was applied in the down-aisle direction to minimize the interference from the loading of the goods. The smaller displacement responses along the width are probably because the columns were connected to each other through bracings for reinforcement. In addition, as a result of the test in the down-aisle direction, a permanent deformation of up

to 84 mm occurred in the top floor (Fig. 3(a)). A permanent deformation of 7.6 mm occurred in the cross-aisle direction, as shown in Fig. 3(b).

The results of the experiment on the vibration characteristics of the storage rack revealed larger displacement responses and permanent deformation in the down-aisle direction than in the cross-aisle direction, due to the influence of the external force. In other words, the resistance of the storage rack to external loads such as earthquakes can be improved by installing reinforcements in the down-aisle direction.

### 2.3 Evaluation of Load Resistance Characteristics of Column-Beam Connections

The results of the experiment in Section 2.2 are in agreement with those of existing studies, which found that the column-beam connections of storage racks in the down-aisle direction were weak. To design reinforcements for this direction, we first studied the load-resistance characteristics of column beam connections. To this end, we connected two columns in the down-aisle direction of the storage rack by using beams (Fig. 1) on top of which the goods would be loaded. To examine the resistance characteristics, we performed an experiment on the load-resistance response of the column-beam connections. The experiment of the connection was conducted based on the static experiment method presented in FEM 10.2.02. The specimen for this experiment was fabricated by connecting a 702-mm-long beam to a 500-mm-long column, as shown in Fig. 4. To prevent the detachment of the beam from the column during the experiment,

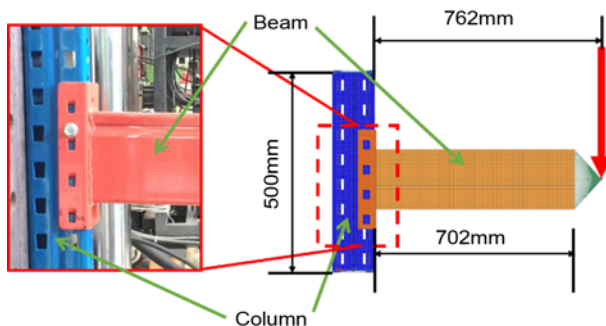


Fig. 4. Specimen for the Load Resistance Experiment

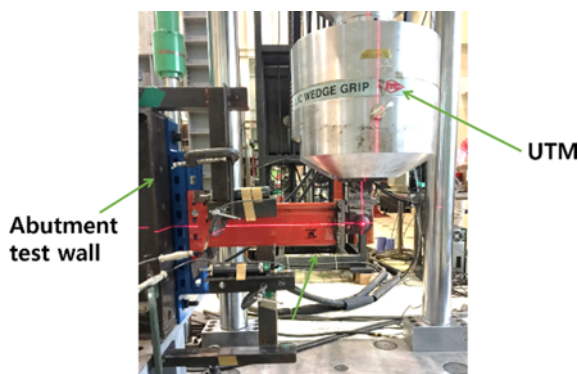


Fig. 5. Apparatus of the Load-Resistance Experiment

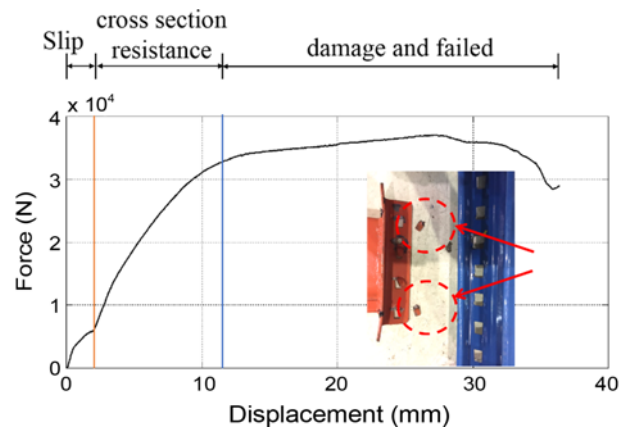


Fig. 6. Shear Force Test Results

we fastened the beam to the second hole of the column using an M8 bolt from the top of the connection.

The experiment was divided into a) a simple one-way load test for examining the shear force of the column-beam connection, and b) a cyclic loading test for investigating the behavioral characteristics of the column-beam connection under cyclic loading. The experiment was conducted by fixing the column to an abutment test wall and the end of the beam to a universal testing machine (UTM), as shown in Fig. 5.

First, during the test to examine the shear force of the column-beam connection, the input load and the generated displacement were measured by applying a force on the specimen in the UTM in the downward direction. The results are shown as a load-displacement curve in Fig. 6.

From Fig. 6, the column-beam connection exhibited responses in three patterns (0 – 2 mm, 2 – 14 mm, and over 14 mm) due to the input load. The first response pattern, the Slip section, occurred from the test start point to 2 mm. In this section, the slope of increasing force decreased. This appears to be because only a small amount of friction force was available for the hooks of the beam to resist the external force while sliding into the holes of the column, even though friction was generated at the beginning of the test from the fastening of the bolt. The next response pattern occurred at 14 mm, which lies beyond the friction resistance section. In this section, the resistive force was generated as the hooks of the beam contacted the walls of the holes in the column, and the load increased with a slope close to a line. The last response pattern occurred at a point beyond 14 mm. The increase in resistance slope was greatly reduced as the latch of the beam and the hole of the column were damaged. Beyond this section, the hooks of the beam were completely cut off, as shown in the graph of Fig. 6. An important section, as confirmed by this test, was the section before the 2-mm point at the beginning of the test. The space between the hooks of the beam and the holes in the column resulted in the displacement of the specimen because it could not resist the external load, which in turn caused the collision between the hooks and the holes due to the strong external force.

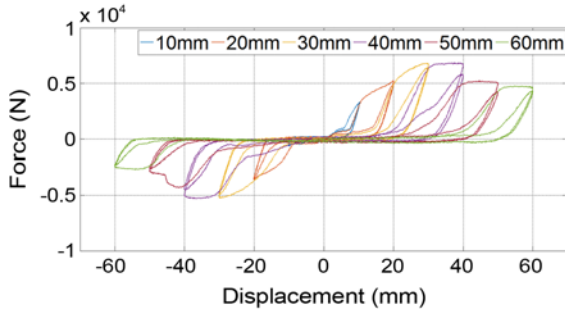


Fig. 7. Cyclic Loading Test Results

Next, in the cyclic loading test, where the column–beam connection motion produced by the external load is examined, the resistive force due to the displacement was measured while repeating displacement control by translating the UTM in the vertical direction under six displacement conditions ( $\pm 10$ ,  $\pm 20$ ,  $\pm 30$ ,  $\pm 40$ ,  $\pm 50$ , and  $\pm 60$  mm). Fig. 7 shows the results of the test.

In Fig. 7, slip and pinching phenomena are observed in all the tests conducted while increasing the displacement by 10 mm. In addition, displacement of the specimen due to the space between the hooks of the beam and the holes in the column, which was confirmed by the shear-force test in Fig. 6, is observed. The occurrence of these phenomena increase with displacement.

### 3. Development of a Viscoelastic Damper System to Reinforce Vulnerable Parts of Storage Racks

#### 3.1 Calculation of Damper's Capacity to Reinforce Vulnerable Parts

From the experiments, we found that the column–beam connections in the down-aisle direction must be reinforced to impart seismic resistance to the storage racks. To develop a viscoelastic damper system for reinforcing the stiffness of the column–beam connections, it is necessary to calculate the capacity of the damper first.

In this study, we calculated the shear force on each floor of the basic storage rack and the corresponding capacity of the viscoelastic damper. Hwang (2002) calculated the modal participation factor of the first mode using the interstory modal drift and thereby the design shear force of a steel structure. In the case of storage racks, however, the maximum displacement of each floor has a larger influence on the falling of goods than the response of the first mode. For this reason, in this study, the shear resistive force was calculated using the maximum interstory drift ratio according to the dynamic load. To calculate the maximum interstory drift ratio according to the dynamic load, a time-history analysis was performed and the continuous movement of the storage rack under seismic loads was examined. The time-history analysis was conducted using the NS component (PGA = 0.283 g) data of the Pohang earthquake that recently rocked South Korea, which were measured at the Pohang (PHA2) observatory. The size and load conditions of the storage rack were applied in the same manner as the shaking table test conducted in Section 2, and the weight of the storage rack (approximately 100 kg) was neglected

because it was much smaller than the load on each floor. The maximum floor drift ratios of the storage rack acquired through the time-history analysis were 1.301, 2.525, and 2.821% for the first, second, and third floors. Evidently, the third floor exhibited the highest value. Maximum story drift ratio was calculated by dividing the maximum displacement from each floor into the height of each floor from the base.

To estimate the capacity of the damper with the reinforcement force (shear force on each floor) capable of responding to the drift ratio of each floor, we calculated the input seismic acceleration as follows:

$$S_a = Z \times I \times C_{sa} \times C_D . \quad (1)$$

In Eq. (1),  $Z$  is the seismic zone factor. We used 0.11, which corresponds to the seismic zone 1 of South Korea, for this study.  $I$  is the risk factor of the average return period of 500 years, i.e., 1. For  $C_{sa}$ , an elastic design spectrum acceleration value of 2.5 normalized with 1.0 g PGA with a 5% damping ratio was used. Finally,  $C_D$  is the damping correction factor, which was calculated using the following equation proposed by the Seismic Design Code of Japan (Otani and Kani, 2002):

$$C_D = \frac{1.5}{1 + 10 \times (\xi / 100)} . \quad (2)$$

In Eq. (2),  $\xi$  is the target damping ratio, and it was set to 20% in this study. The maximum floor drift ratio was calculated through the time-history analysis. The participation factor (PF) is a scalar value that determines the degree of system parameters affecting the vibration mode formation of a linear system, and is generally calculated for the mode of the system. In this study, the maximum interstory drift ratio calculated from maximum floor drift ratio was applied by recognizing the importance of the displacement of each floor rather than the mode of the storage rack. The PF for the maximum response is (Sharad and Suhasini, 2015)

$$PF = \frac{\sum_i^n m_i \Delta_{i, \max, f}}{\sum_i^n m_i \Delta_{i, \max, f}^2} . \quad (3)$$

In Eq. (3),  $m_i$  is the mass of the  $i^{\text{th}}$  floor and  $\Delta_{i, \max, f}$  is the maximum drift of the  $i^{\text{th}}$  floor. The PF calculated from Eq. (3) was substituted into Eq. (4), to derive the acceleration of each floor. This value was then substituted into Eq. (5) to calculate the design lateral force:

$$A_i = PF \times \Delta_{i, \max, f} \times S_a , \quad (4)$$

$$F_i = m_i \times A_i . \quad (5)$$

The design lateral force of each floor calculated from Eq. (5) is the lateral force of each floor. The lateral force of the second floor is affected by that of the third floor, and the lateral force of the first floor is affected by those of the second and third floors. Finally, the design shear force was calculated by adding the

**Table 2.** Major Variables for the Calculation of the Damper Capacity

	1 <sup>st</sup>	2 <sup>nd</sup>	3 <sup>rd</sup>
Maximum interstory drift ratio (between floors) ( $\Delta_{max}$ )	1.301	1.224	0.296
Mass ( $m$ )	1,200 kg		
Seismic zone factor ( $Z$ )	0.11		
Importance factor ( $I$ )	1		
Elastic design spectral acceleration ( $C_{sa}$ )	2.5		
Damping modification factor ( $C_D$ )	0.5		
Target damping ratio ( $\xi$ )	20%		

**Table 3.** Design Shear Force on Each Floor of the Storage Rack

	1 <sup>st</sup>	2 <sup>nd</sup>	3 <sup>rd</sup>
Design floor shear force (kN)	39.29	35.17	18.12

design lateral force of each floor. Table 2 summarizes the values of the variables used to calculate the design shear force. Table 3 lists the calculated design shear force on each floor of the storage rack.

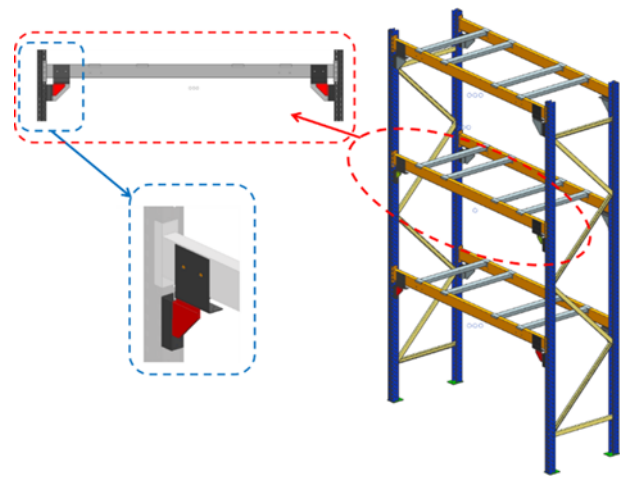
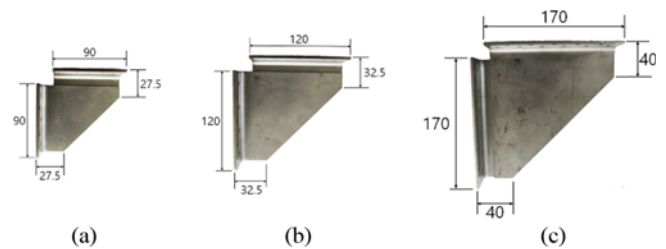
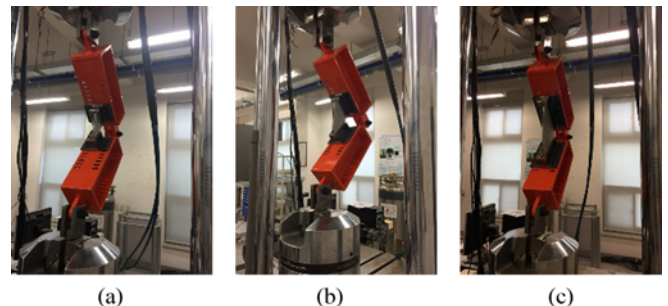
The capacity of the viscoelastic damper to reinforce the vulnerable part (column–beam connection) of the storage rack in the down-aisle direction was designed to have the control force required to respond to the shear force in Table 3. The viscoelastic damper was conceptualized and developed as a triangular shape, to prevent it from interfering with the loading of goods. We assumed that the force that acted on the damper was applied at an angle of  $45^\circ$  as the damper is located at the column–beam connection. To prevent the integral behavior of the floors due to excessive control, the control force was selected such that it did not exceed 19.5 kN, which corresponds to 50% of the design shear force of the first floor and is the maximum shear force of the storage rack in Table 3. Since it is possible to install four dampers on each floor, the maximum capacity of a damper was determined as 5 kN.

### 3.2 Viscoelastic Damper Fabrication and Performance Verification

The viscoelastic damper was designed and fabricated based on the design shear force on each floor from Table 3. The down-aisle direction of the storage racks is the direction in which goods on pallets are loaded using mechanical equipment. Thus, if interferences such as a collision occur during the loading, the goods may fall. To circumvent this problem, we designed a small damper that can be attached without the operational interruption of storage racks, while reinforcing both the down-aisle direction and the column–beam connection, as shown in Fig. 8.

The damper reinforces beams and columns of vulnerable parts using a simple jig, as shown in Fig. 8. Because it is attached to a column–beam connection, up to four dampers can be used on each floor. The control force is adjusted by varying the number of dampers.

The viscoelastic damper system uses 3M's ISD-111 (VE polymer)

**Fig. 8.** Damper for Reinforcing Vulnerable Parts**Fig. 9.** Viscoelastic Damper Developed in Three Sizes: (a) A Size (90 mm), (b) B Size (120 mm), (c) C Size (170 mm)**Fig. 10.** Load Resistance Test of the Viscoelastic Dampers: (a) A Size (90 mm), (b) B Size (120 mm), (c) C Size (170 mm)

acrylic polymer material for its excellent resilience. The control force of the damper can be adjusted by varying the width of the material. Based on the characteristics of this material, which exhibits constant control force despite partial failure, the damper was developed in three sizes according to the capacity requirement (Fig. 9).

The mechanical performance of the dampers was tested in a UTM. In this test, the displacement was varied by  $\pm 2$ ,  $\pm 4$ , and  $\pm 6$  mm, to examine the control force with respect to the displacement.

As shown in Fig. 10, the test was conducted by attaching each damper to the jig fabricated for the test and connecting the end of the jig to the UTM. The graphs below show the performance test results of each damper using force–displacement curves. From Fig. 11, dampers of sizes A, B, and C exhibit maximum forces of

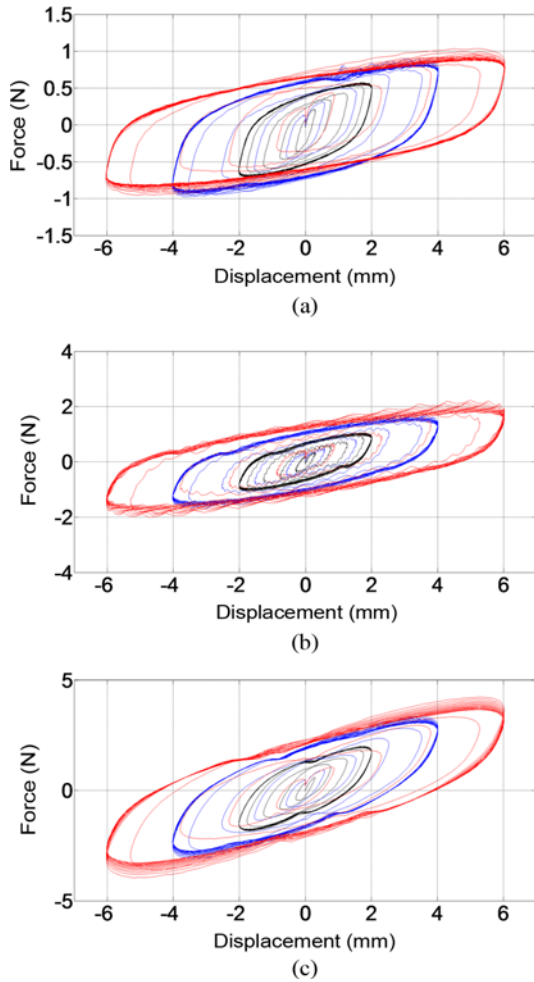


Fig. 11. Test Results of Mechanical Performance of Viscoelastic Dampers: (a) Load–Displacement Curves of Size A (90 mm), (b) Load–Displacement Curves of Size B (120 mm), (c) Load–Displacement Curves of Size C (170 mm)

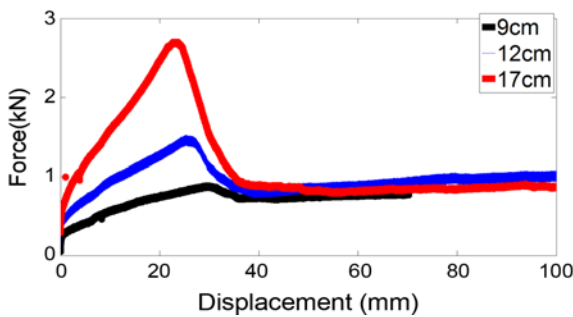


Fig. 12. Limit State Test of the Viscoelastic Dampers

1, 2, and 4.5 kN, respectively. For each damper, the control force increases with displacement.

To investigate its characteristics, the damper material was subjected to a limit state test. In the test, the load at the limit state was examined by controlling the displacement of the dampers at a rate of 10 mm/min. Fig. 12 illustrates the plot of force–displacement responses. The three dampers maintained a control

force of approximately 0.7 kN until complete failure after yielding. For the smallest damper of size A, complete failure occurs at a displacement of 70.28 mm, and a control force of 0.7 kN is maintained until the two plates, to which the viscoelastic material was attached, are detached. In other words, the dampers should be effective in preventing a collapse because they maintained a constant control force until failure, despite yielding due to strong external force.

#### 4. Shaking Table Test for Performance Verification of Viscoelastic Dampers

##### 4.1 Shaking Table Test Method for the Storage Rack

In storage racks with multiple floors, each floor will require a different magnitude of resistive force to counter the seismic vibration, and excessive reinforcement of certain floors will cause stress on other floors. This excessive stress will lead to failure. Therefore, it is important to select viscoelastic dampers that are compatible with each floor in terms of capacity.

The calculations of the damper capacity required for reinforcing vulnerable parts in Section 3.1 revealed the first floor as enduring the largest shear force, followed by the second and third floors. However, the third floor had the largest displacement, which means that goods located on the higher floors can cause collisions with columns due to large displacements due to external forces, which can damage the columns. For this reason, we decided to install the size C damper with the largest capacity on the third floor. In addition, size B damper was installed on the first floor, which has a larger design shear force than the second floor, and the size A damper on the second floor, as shown in Fig. 13.

A shaking table test was conducted to examine the vibration-reducing performance of the storage rack reinforced with the viscoelastic damper systems (Fig. 13). The storage rack may have a warping motion due to horizontal seismic force. However the viscoelastic damper was developed only for the down-aisle

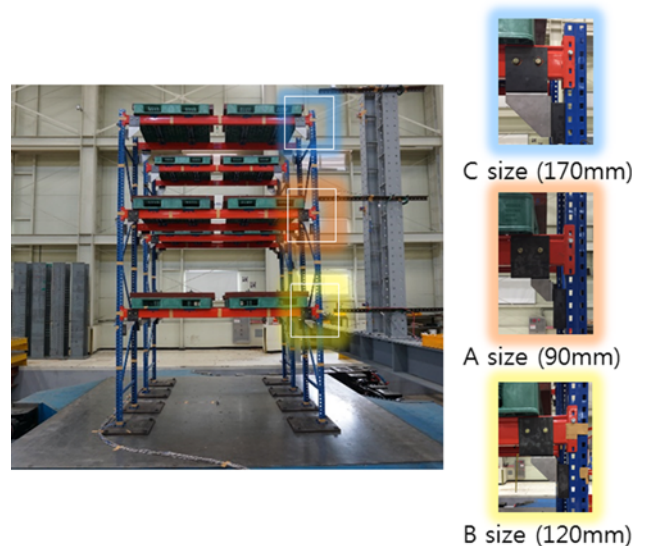


Fig. 13. Installation Positions of the Viscoelastic Dampers



direction, therefore warping effect reduction of the storage rack due to the external force were not considered in this research.

The test was conducted using the same seismic waveform as in the experiment on the behavioral characteristics of a basic storage rack under seismic vibration (Section 2). In the shaking table test, however, uniaxial excitation was applied in the down-aisle direction because the purpose of the viscoelastic dampers is to reinforce storage racks in that direction. The test was conducted both under the basic condition (BC) without the installation of dampers and under the reinforced condition (RC) with the installation of dampers at the column–beam connections.

#### 4.2 Verification of Seismic Reduction Performance of the Viscoelastic Dampers

The effect of the viscoelastic damper system in improving the seismic performance of the rack was evaluated by comparing the vibration displacement responses of each floor obtained through the shaking table test. The responses of each floor were measured by installing displacement sensors at the column positions adjacent to the right column–beam connections on the first, second, and third floors. Fig. 14 plots the displacement responses of each floor obtained from the shaking table test conducted under BC with respect to time.

As shown in Fig. 14, for the basic storage rack, differences in displacement between the floors begin to occur approximately five seconds after the start of the test, and then increase approximately from the 10 s. In addition, the third floor represented by the blue line exhibited a displacement of up to 200 mm and a permanent deformation of 44.46 mm. Fig. 15 shows the displacement responses of each floor obtained from the shaking table test conducted under the RC.

As shown in Fig. 15, for the reinforced storage rack, differences

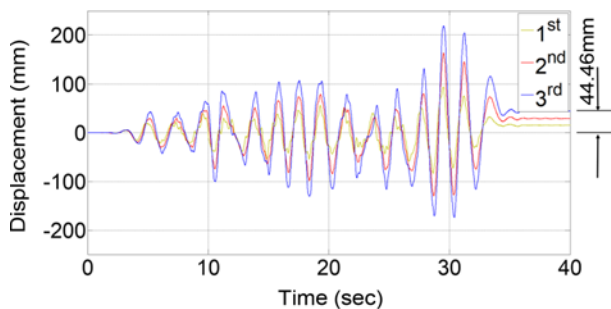


Fig. 14. Displacement Responses of Each Floor of the Basic Storage Rack

in displacement between the floors begin to occur approximately 5 s after the start of the test as with the basic storage rack. In Figs. 14 and 15, however, such differences and the displacement responses of each floor are smaller compared to the basic storage rack. In particular, while the basic storage rack exhibits large displacements approximately 10 s after the start of the test, the reinforced storage rack does not show any significant increase in the displacements of each floor and between the floors, because the displacement of each floor was properly controlled amid the increasing external force.

To compare the test results of the BC in Fig. 14 with those of the RC in Fig. 15, the maximum displacement and maximum permanent deformation of each floor are plotted in Fig. 16. Table 4 also shows the maximum displacement and permanent deformation of each floor for the basic and reinforced storage racks. In Fig. 17, the viscous damping values of the storage racks are estimated by half-power bandwidth method using random wave excitation test results. Trial-and-error curve-fit convergence was performed using transmissibility function of input and response

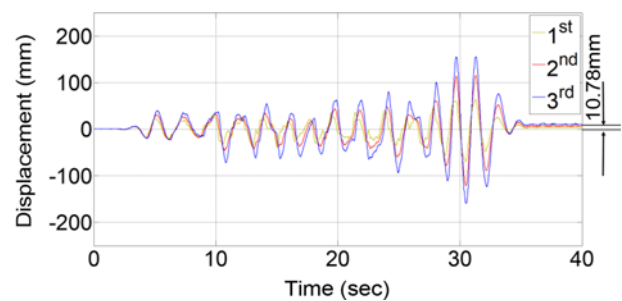


Fig. 15. Displacement Responses of Each Floor of the Reinforced Storage Rack

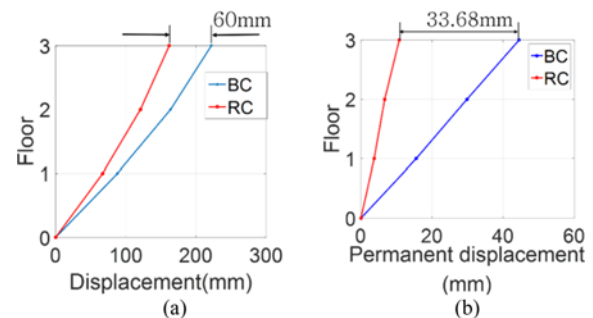
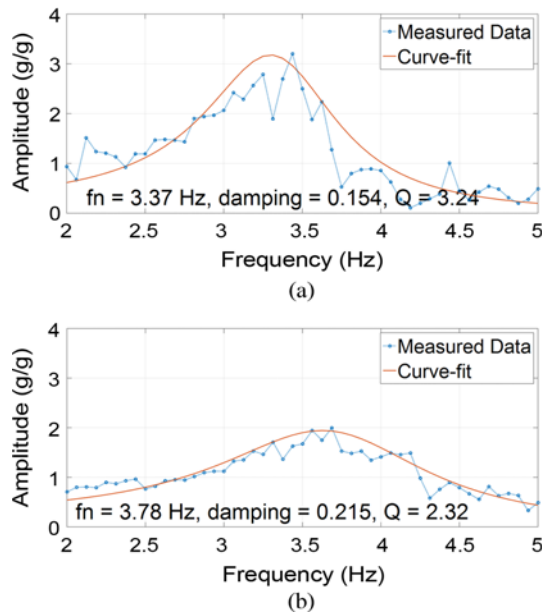


Fig. 16. Comparison of the Shaking Table Test Results of the Storage Racks: (a) Maximum Displacement by Floor, (b) Permanent Deformation by Floor

Table 4. Comparison of the Shaking Table Test Results of the Storage Racks

	Maximum displacement (mm)			Permanent deformation (mm)		
	1 <sup>st</sup>	2 <sup>nd</sup>	3 <sup>rd</sup>	1 <sup>st</sup>	2 <sup>nd</sup>	3 <sup>rd</sup>
Basic storage rack	88	164	222	15.56	29.82	44.46
Reinforced storage rack	67	121	162	3.72	6.69	10.78
Reduction rate (%)	23.9	26.2	27	76.1	77.6	75.8



**Fig. 17.** Comparison of Damping in 3rd Floor: (a) Basic Storage Rack, (b) Reinforced Storage Rack

acceleration measurements. The target frequency is from 2.0 to 5.0 Hz where the 1st mode frequency exists.

From Fig. 16 and Table 4, the viscoelastic damper system reduces the maximum displacement of the storage rack due to the seismic load by 60 mm, which is related to the fall of the product and, despite the difference between floors, shows a damping effect that exceeds the 20% target as shown in Fig. 17. In the case of permanent deformation that contributes to the collapse of storage racks, the maximum permanent deformation of the regular storage rack (without damper) was reduced by 33.7 mm. With the new damper system, each floor witnessed more than 75% reduction in permanent deformation compared with the basic storage rack.

## 5. Conclusions

In this study, we developed a viscoelastic damper system for reinforcing the vulnerable parts of a storage rack and improve its resistance to seismic loads, which otherwise cause loss of life and property. First, the elements of the storage rack that require reinforcement were identified through a shaking table test. The test also allowed us to investigate the vibration characteristics of storage racks under an external force. We confirmed that the down-aisle direction (length) is more vulnerable than the cross-aisle direction. With the same test, we examined the structural members and found that the column–beam connections of the rack must be reinforced to counter the external forces. The shear force on each floor was calculated. Three dampers of different capacities were designed to meet the shear force results. We then determined the positions on each floor where the three viscoelastic damper systems must be placed to absorb the vibrations, taking

into account the design shear force on the storage rack due to the external force and the maximum floor drift obtained through a time-history analysis. In addition, another shaking table test was conducted to examine the vibration reduction effect in the reinforced storage rack. The results of this study are as follows.

1. An analysis of the behavioral characteristics of a conventional storage rack and a series of cyclic loading tests on the column–beam connection found a relatively large displacement and a more severe permanent deformation in the down-aisle direction than in the cross-aisle direction where members are reinforced with bracings. The space present in the column–beam connections, which are applied for easy height adjustment, causes the connections to behave abnormally under external force. In other words, the column–beam connections in the down-aisle direction must be reinforced for seismic resistance.
2. The capacity of the damper in the new system was determined by calculating the shear force on each floor based on the maximum interstory drift ratio, which in turn was estimated through a time-history analysis. In addition, the geometry and installation method that would allow the dampers to function without interrupting the operation of the storage racks and the loading of goods were proposed. The cyclic loading test results confirmed that the viscoelastic damper exhibited an increase in control force with displacement. Moreover, the damper maintained a constant control force until failure even after it had yielded.
3. A shaking table test was conducted to examine the vibration-reduction performance of the viscoelastic damper system under external force. The system reduced the displacement of each floor due to the external force, which is related to the falling of goods, by up to 27%. It also reduced the permanent deformation, which is related to the collapse of storage racks, by up to 77%, confirming its displacement control performance.

The damper system successfully reinforced the members along the down-aisle direction (length) and the column–beam connections, which are the vulnerable elements of a storage rack experiencing lateral loads. The system achieved the objective of this study by exhibiting its displacement reduction performance, which can prevent goods from falling and storage racks from collapsing under an external force. The damper can be easily installed without interrupting the operation of storage racks, and it can be used to secure small groups of storage racks due to its affordability and compactness.

## Acknowledgments

This research was supported by National Research Foundation of Korea through funding from the Ministry of Education (Project No: NRF-2018R1A6A1A03025542 and NRF-2019R1I1A1A01049701). Many appreciation and acknowledgements go to the National Research Foundation who made this research possible.

## ORCID

Gwanghee Heo  <https://orcid.org/0000-0003-2629-1726>  
 Hyoungsuk Choi  <https://orcid.org/0000-0002-1340-9724>  
 Eunrim Baek  <https://orcid.org/0000-0003-1041-6096>  
 Chunggil Kim  <https://orcid.org/0000-0002-0431-0300>

## References

- Abdel-Jaber M, Beale RG, Godley MHR (2005) Numerical study on semi-rigid racking frames under sway. *Computers and Structures* 83(28-30):2463-2475, DOI: [10.1016/j.compstruc.2005.03.020](https://doi.org/10.1016/j.compstruc.2005.03.020)
- AC156:2010 (2015) Acceptance criteria for seismic certification by shake-table testing of nonstructural components. International Code Council Evaluation Service
- ANSI MH16.1 (2012) Specification for the design, testing and utilization of industrial steel storage racks. Rack Manufacturers Institute, Charlotte, NC, USA
- Bajoria KM, Talikoti RS (2006) Determination of flexibility of beam to column connectors used in thin walled cold formed steel pallet racking systems. *Thin-Walled Structures* 44(3):372-380, DOI: [10.1016/j.tws.2006.01.007](https://doi.org/10.1016/j.tws.2006.01.007)
- Beale RG, Godley MHR (2004) Sway analysis of spliced pallet rack structures. *Computers and Structures* 82(23-26):2145-2156, DOI: [10.1016/j.compstruc.2004.03.063](https://doi.org/10.1016/j.compstruc.2004.03.063)
- Bernuzzi C, Castiglioni CA (2001) Experimental analysis on the cyclic behaviour of beam-to-column joint in steel storage pallet racks. *Thin-Walled Structures* 39(10):841-859, DOI: [10.1016/S0263-8231\(01\)00034-9](https://doi.org/10.1016/S0263-8231(01)00034-9)
- Bograd S, Reuss P, Schmidt A, Gaul L, Mayer M (2011) Modeling the dynamics of mechanical joints. *Mechanical Systems and Signal Processing* 25(8):2801-2826, DOI: [10.1016/j.ymssp.2011.01.010](https://doi.org/10.1016/j.ymssp.2011.01.010)
- Building Seismic Safety Council (2009) NEHRP recommended provisions for the development of seismic regulations for new buildings. Building Seismic Safety Council, Federal Emergency Management Agency, Washington DC, USA
- Castiglioni (2016) Dynamic full-scale tests. Shaking table tests on steel pallet racks. *Seismic Behavior of Steel Storage Pallet Racking Systems*, 357-437
- Castiglioni CA, Panzeri N, Brescianini JC, Carydis P (2003) Shaking table tests on steel pallet racks. *Proceedings of the Conference on Behaviour of Steel Structures in Seismic Areas-Stessa*, Naples, Italy, 775-781
- Chen CK, Scholl RE, Blume JA (1980a) Seismic study of industrial storage racks. Report prepared for the National Science Foundation and for the Rack Manufacturers Institute and Automated Storage and Retrieval Systems (sections of the Material Handling Institute). URS/John A. Blume & Associates, San Francisco, CA, USA
- Chen CK, Scholl RE, Blume JA (1980b) Earthquake simulation tests of industrial steel storage racks. *Proceedings of the Seventh World Conference on Earthquake Engineering*, Istanbul, Turkey, 379-386
- de Lima LRO, de Andrade SAL, da S Vellasco PCG, da Silva LS (2002) Experimental and mechanical model for predicting the behavior of minor axis beam-to-column semi-rigid joints. *International Journal of Mechanical Sciences* 44(6):1047-1065, DOI: [10.1016/S0020-7403\(02\)00013-9](https://doi.org/10.1016/S0020-7403(02)00013-9)
- EN 1993-1-3 (2006) Eurocode 3—Design of steel structures—Part 1–3: General rules—Supplementary rules for cold-formed members and sheeting. EN 1993-1-3, European Committee for Standardization, Brussels, Belgium
- EN 15512 (2009) Steel static storage systems – Adjustable pallet racking systems – Principles for structural design. EN 15512, European Committee for Standardization, Brussels, Belgium
- Eriten M, Kurt M, Luo G, McFarland MD, Bergman LA, Vakakis AF (2013) Nonlinear system identification of frictional effects in a beam with a bolted joint connection. *Mechanical Systems and Signal Processing* 39(1-2):245-264, DOI: [10.1016/j.ymssp.2013.03.003](https://doi.org/10.1016/j.ymssp.2013.03.003)
- FEM 10.2.02 (2000) The seismic design of static steel pallet racks. FEM 10.2.02, FEM Racking and Shelving Product Group, Brussels, Belgium
- FEM 10.2.08 (2010) Recommendations for the design of static steel pallet racks under seismic conditions. FEM 10.2.08, FEM Racking and Shelving Product Group, Brussels, Belgium
- FEMA 460 (2005) Seismic considerations for steel storage racks located in areas accessible to the public. FEMA 460, National Institute of Building Sciences, Washington DC, USA
- Filiatrault A, Higgins PS, Wanitkorkul A, Courtwright J (2007) Experimental stiffness of pallet type steel storage rack tier drop connectors. *Practice Periodical on Structural Design and Construction* 12(4):210-215, DOI: [10.1061/\(ASCE\)1084-0680\(2007\)12:4\(210\)](https://doi.org/10.1061/(ASCE)1084-0680(2007)12:4(210))
- Hwang JS (2002) Seismic design of structures with viscous dampers. International Training Programs for Seismic Design of Building Structures
- Jovanović Đ, Žarković D, Vukobratović V, Bruić Z (2019) Hysteresis model for beam-to-column connections of steel storage racks. *Thin-Walled Structures* 142(2019):189-204, DOI: [10.1016/j.tws.2019.04.056](https://doi.org/10.1016/j.tws.2019.04.056)
- KBC (2016) Korean building code-Structural. Architectural Institute of Korea, Seoul, Korea
- Kozłowski A, Słeczka L (2004) Preliminary component method model of storage rack joint. *Proceedings of the Connections in Steel Structures*, Amsterdam, The Netherlands
- Krawinkler H, Cofie NG, Astiz MA, Kircher CA (1978) Experimental study on the seismic behavior of industrial storage racks. Report No. 41, The John A. Blume Earthquake Engineering Center, Department of Civil Engineering, Stanford University, Stanford, CA, USA
- Kwarteng KO, Besle Robert, Godley MHR, Thomson SD (2012) The effects of seismic loading on pallet rack semi-rigid joints. *Proceedings of the eleventh international conference on computational structures technology*, September 4-7, Dubrovnik, Croatia, DOI: [10.4203/ccp.99.21](https://doi.org/10.4203/ccp.99.21)
- Markazi FD, Beale RG, Godley MHR (1997) Experimental analysis of semi-rigid boltless connectors. *Thin-Walled Structures* 28(1):57-87, DOI: [10.1016/S0263-8231\(97\)00003-7](https://doi.org/10.1016/S0263-8231(97)00003-7)
- Otani S, Kani N (2002) Japanese state of practice in design of seismically isolated buildings. The fourth US-Japan workshop on performance-based earthquake engineering methodology for reinforced concrete building structures, October 22–24, Toba, Japan
- Shah SNR, Ramli Sulong NH, Shariati M, Jumaat MZ (2015) Steel rack connections: Identification of most influential factors and a comparison of stiffness design methods. *Plos One* 10(10), DOI: [10.1371/journal.pone.0139422](https://doi.org/10.1371/journal.pone.0139422)
- Sharad M, Suhasini M (2015) Seismic design of RC buildings: Theory and practice. Springer, Berlin, Germany
- Słeczka L, Kozłowski A (2007) Experimental and theoretical investigations of pallet racks connections. *Advanced Steel Construction* 3(2):607-627, DOI: [10.18057/IJASC.2007.3.2.6](https://doi.org/10.18057/IJASC.2007.3.2.6)